LA-UR-15-21451
Approved for public release; distribution is unlimited.

Title: Using Richtmyer-Meshkov Instabilities to Estimate Metal Strength at Very High Rates

Author(s): Prime, Michael Bruce
Buttler, William Tillman
Sjue, Sky K.
Jensen, Brian J.
Mariam, Fesseha Gebre
Oro, David Michael
Pack, Cora Lynn
Stone, Joseph B.
McNeil, Wendy Vogan
Tupa, Dale

Intended for: SEM 2015 Annual Conference and Exposition on Experimental and Applied Mechanics, 2015-06-08/2015-06-11 (Costa Mesa, California, United States)

Issued: 2015-02-26

Final Reference is a book chapter in the conference proceedings series:

Prime, M. B., Buttler, W. T., Sjue, S. K., Jensen, B. J., Mariam, F. G., Oró, D. M., Pack, C. L., Stone, J. B., Tupa, D., and Vogan-McNeil, W., 2016, "Using Richtmyer–Meshkov Instabilities to Estimate Metal Strength at Very High Rates," Dynamic Behavior of Materials, Volume 1, B. Song, L. Lamberson, D. Casem, and J. Kimberley, eds., Springer International Publishing, pp. 191-197.

Available at: http://dx.doi.org/10.1007/978-3-319-22452-7_27

Using Richtmyer-Meshkov Instabilities to Estimate Metal Strength at Very High Rates

Michael B. Prime, William T. Buttler, Sky K. Sjue, Brian J. Jensen, Fesseha G. Mariam, David M. Oró, Cora L. Pack, Joseph B. Stone, Dale Tupa, Wendy Vogan-McNeil
Los Alamos National Laboratory, P.O. Box 1663, Los Alamos, NM 87545

ABSTRACT

Recently, Richtmyer-Meshkov instabilities (RMI) have been proposed for studying strength at strain rates up to 10^7/s. RMI experiments involve shocking a metal interface that has geometrical perturbations that invert and grow subsequent to the shock. As these perturbations grow, their growth may arrest, or they may grow unstably and eventually fail. The experiments observe the growth and arrest to study the specimen's yield (deviatoric) strength. Along these lines we first review some RMI experimental results on Cu. Next, the paper presents explicit Lagrangian simulations used to help interpret the Cu RMI results and infer the strength, i.e. flow stress, of the target metal. A Preston-Tonks-Wallace (PTW) constitutive model is modified to be more accurate at the strain rates accessed in the experiment. The advantages and disadvantages of RMI, as compared to the Rayleigh-Taylor (shockless) instabilities that are used more commonly to infer strength, are discussed. The advantages of using simple velocimetry measurements in place of radiography is also discussed.

Keywords: Richtmyer-Meshkov instabilities, shock, high strain rate, strength, Rayleigh-Taylor

INTRODUCTION

Rayleigh Taylor (RT) instabilities have long been used to infer material strength [1-3] and recently have been instrumental in developing sophisticated constitutive models for the high-pressure, high-rate regimes accessed in such experiments [4,5]. Figure 1 illustrates a typical RT experiment. In the RT geometry, gaseous detonation products from a high explosive (HE) expand across a vacuum gap and shocklessly accelerate a sample that has initial geometric perturbations. Strength (meaning resistance to deviatoric, i.e., shear, deformation) moderates the growth rates of the instabilities. The perturbation growth rates, measured experimentally with radiography, are then used to indirectly estimate the strength of the sample at very high strain rates.

Only more recently, Richtmyer-Meshkov Instabilities (RMI) have also been shown to be sensitive to strength at strain rates up to 10^7/s [6-13]. Figure 2 illustrates an RMI experiment in the configuration fielded in recent experiments [8,9]. In contrast to the RT experiments, the sample in the RMI experiment is loaded by a shock rather than by a shockless acceleration. Also, strength is determined by testing different sized perturbations and finding those where strength *arrests* the instability growth, as compared to measuring growth rates as is done in RT experiments.

Figure 2 shows an RMI experiment for the case of the perturbations on the free surface opposite of the shock loading (Atwood number A_t = -1). This free surface configuration is the only published experimental implementation of RMI for strength measurements [8,9,14] maybe partly because it is easier to diagnose a free surface but also because it studies the question of ejecta from a shocked surface [9,14-19]. The original idea for RMI strength measurements [6,7] described a configuration where the perturbations were an inner surface in the experiment (e.g., A_t = +1), which follows the more traditional fluid mechanics view of RMI, but are more difficult to experimentally field and diagnose. Note that in the configuration of Figure 2, the shock releases quickly from the free surface, so most of the spike growth and arrest occurs at low pressure. In the traditional A_t = +1 configuration, the shock pressure is supported during spike growth and arrest.

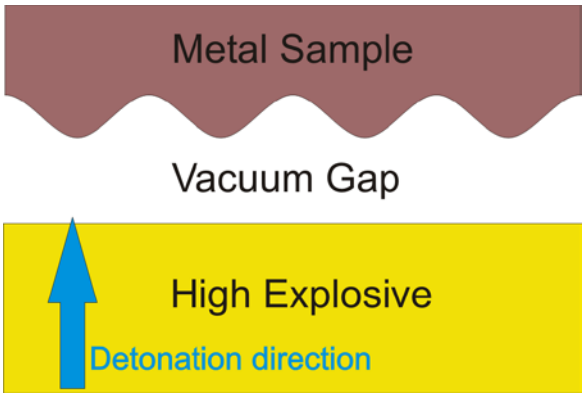

Figure 1. Schematic of Rayleigh-Taylor instability experiment. The HE detonation products *shocklessly* accelerate the perturbed surface of the sample.

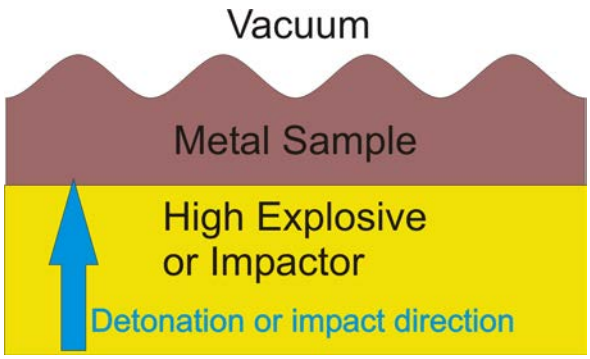

Figure 2. Schematic of a Richtmyer-Meshkov instability experiment (for Atwood = -1). The perturbed surface of the sample is accelerated by a *shock* from an impact or from HE detonation.

Experiment

A set of experiments performed in the Figure 2 configuration, to study strength in Cu, are analyzed using hydrodynamic modeling to continue work from a previous study [13]. The new experiments reported here are virtually identical to a set of experiments reported in detail elsewhere [9,14]. The experiment uses a plane wave lens and a momentum trapping target to approximate the ideal conditions illustrated in Figure 2. The experiments were diagnosed using proton radiography [20] and Photon Doppler Velocimetry (PDV) [21]. The target uses OFHC Cu in the half-hard state with a total thickness of 8 mm. The sine wave perturbations have a wavelength, λ, of 550 μm. In the new study, five initial perturbation amplitudes were studied, η_0 = 28-55 μm, to give non-dimensional $\eta_0 k$ (where $k = 2\pi/\lambda$) of 0.32, 0.38, 0.45, 0.53 and 063. These $\eta_0 k$'s were chosen to better constrain the previous results [9,14], where a $\eta_0 k$ = 0.35 case had significant spike growth and arrest, but where the next bigger $\eta_0 k$, 0.75 had unstable spike growth. By further mapping the $\eta_0 k$ regime where there is spike growth that arrests, the regime with the most sensitivity to strength, it is hoped to refine the strength information that can be extracted.

Modeling

Continuum simulations were performed using Flag, a Lagrangian hydrodynamics code [22,23]. The simulations were similar to those used in a previous study [13], but with some updates. Each simulation used a two-dimensional plane strain mesh that modeled two full wavelengths of the perturbation, see Figure 3, and had constraints on the top and bottom to prevent vertical displacements, effectively assuming periodic behavior.

The PBX 9501 HE was modeled using a JWL equation of state with constants from Dobratz [24] and programmed burn. The Cu sample was modeled using SESAME tabular equation of state 3336 [25], a Preston-Wonks-Wallace (PTW) deviatoric strength model [26], and the Tonks ductile damage and failure model [27-30]. The Tonks damage model was previously calibrated for Cu using flyer plate spall data and, notably, incipient spall data with experimentally measured distributions of porosity [31].

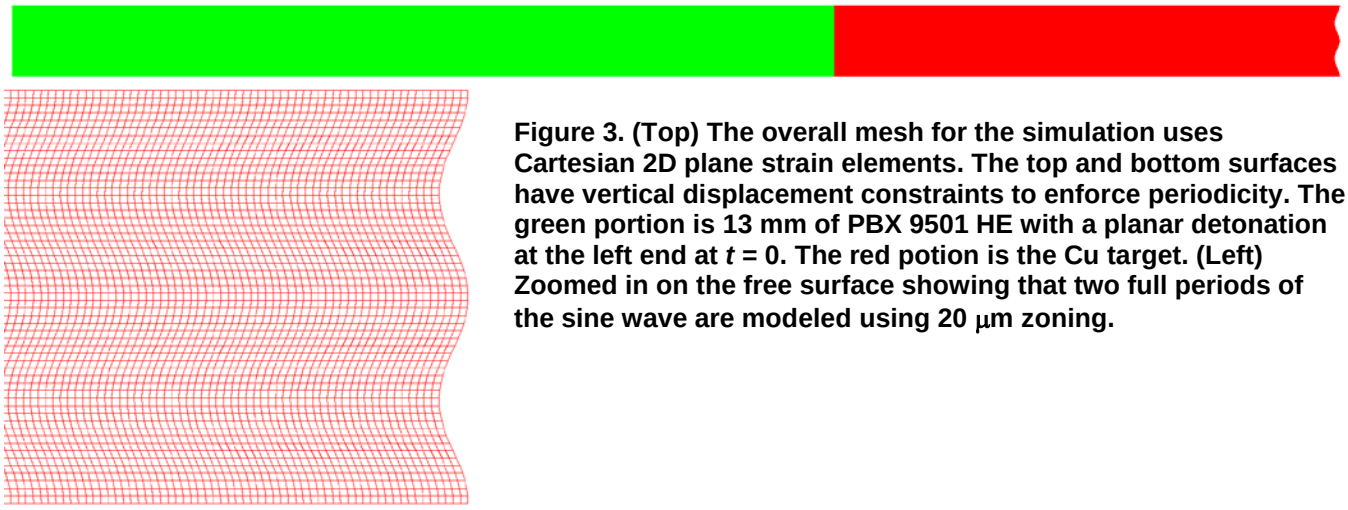

Figure 3. (Top) The overall mesh for the simulation uses Cartesian 2D plane strain elements. The top and bottom surfaces have vertical displacement constraints to enforce periodicity. The green portion is 13 mm of PBX 9501 HE with a planar detonation at the left end at *t* = 0. The red potion is the Cu target. (Left) Zoomed in on the free surface showing that two full periods of the sine wave are modeled using 20 μm zoning.

Results

We present results from the $\eta_0 k = 0.45$ case, which arrested, because the cases with $\eta_0 k \geq 0.53$ grew unstably. Figure 4 shows several snapshots from the simulation, with times taken relative to detonation of the HE. At 2.9 μs, the rightward moving shock is about to reach the free surface with the initial perturbations. At 3.0- and 3.1-μs the perturbations invert and grow as the shock releases at the vacuum-surface interface. By 3.2 μs the perturbation growth has essentially arrested and the damage model has predicted some porosity growth caused by tension. The porosity growth can be seen by the regions with densities below the nominal.

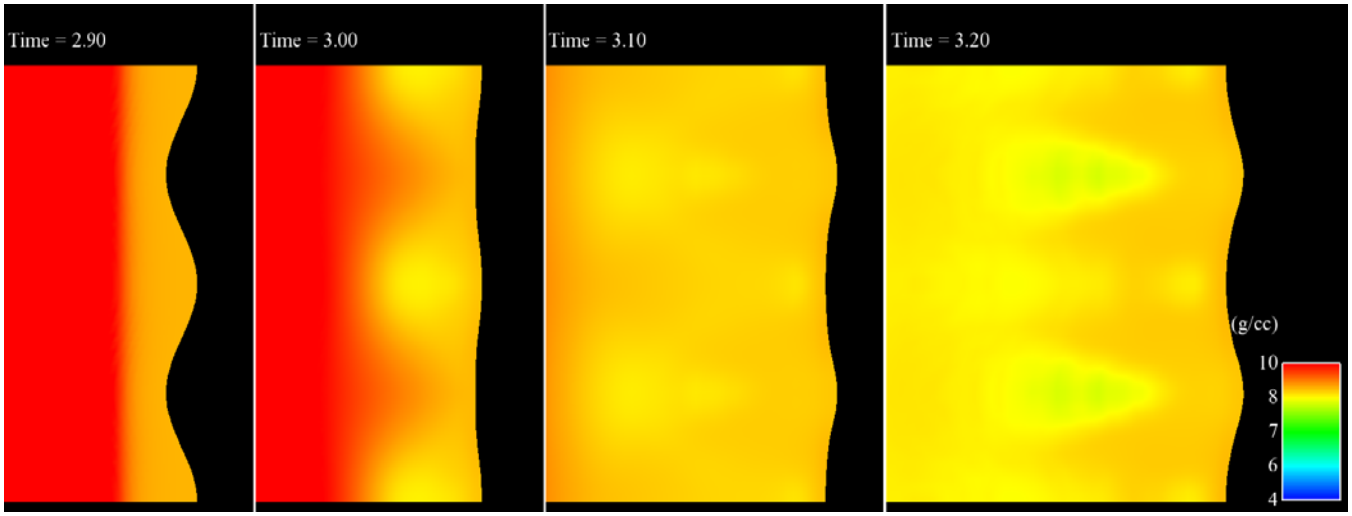

Figure 4. Model snapshots of the inversion, growth and arrest of Richtmyer-Meshkov instabilities in Cu. The density coloration shows the incoming shock, free surface release, and the beginnings of porosity development from tension.

Figure 5 shows the PDV-measured velocities for $\eta_0 k = 0.45$. The PDV spot size is sufficient to see a full perturbation wavelength, so the plotted velocity spectra includes the high and low spots of the final perturbations, also known as the spikes and bubbles. The peak velocity is that of the spike, which decays back to the 1.5 mm/μs level of the overall free surface, thus indicating arrest of the spike growth. Figure 6 shows the spike velocity, extracted from the data of Figure 5, compared with the results of the hydrodynamic simulation. The simulation has predicted too low of a spike velocity. The total predicted spike growth, which equals the area between the spike velocity curve and the velocity of the overall free surface, is therefore significantly under predicted. Those discrepancies occur because the PTW strength model is too strong is this regime.

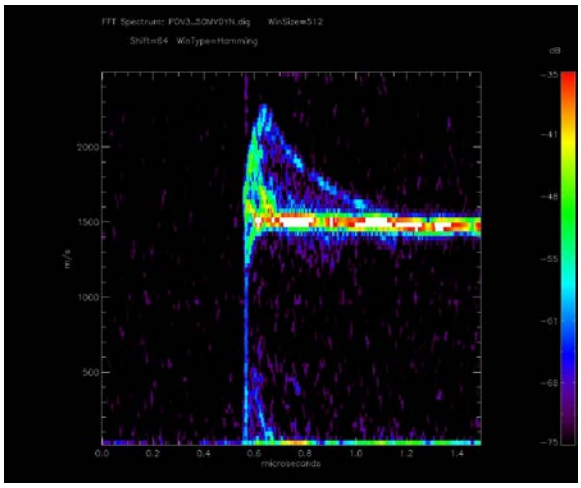

Figure 5. Experimentally measured velocity spectra for the $\eta_0 k$ = 0.45 case. The PDV probes simultaneously measures all the surface in its field of view, with the maximum value in this plot corresponding to the spike.

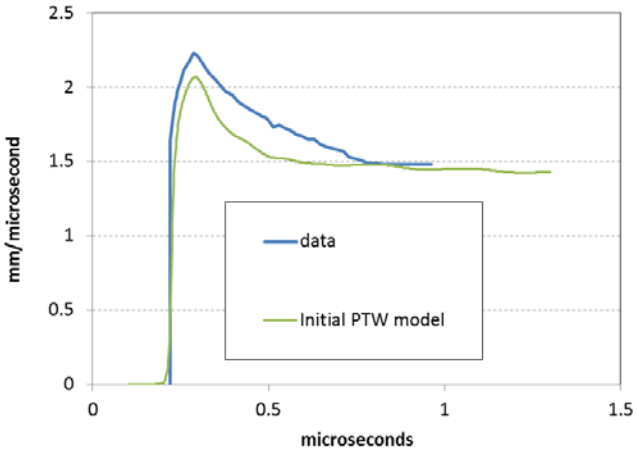

Figure 6. The initial model prediction underestimates the velocity and therefore the total spike growth, which indicates that the model has the Cu too strong.

The PTW model was calibrated using quasi-static and Hopkinson bar stress-strain data taken at rates from 10^{-3}/s to 2800/s and temperatures from 77 K to 473 K. The hydrodynamic simulation of this RMI experiment indicated that the spike growth and arrest occurs mostly at strain rates between 1.5×10^6/s and 6.0×10^6/s. The analysis of the previous RMI experiments in this series [9], which includes a modification to the Piriz equation [7], estimated an average flow strength of 520 MPa. In this 10^6/s strain rate regime, the PTW model is transitioning from a thermally-activated dislocation glide regime for modest strain rates (say up to the calibration data of about 10^4/s) to the strong shock (phonon drag) regime of 10^9/s and up. There is no experimental basis for the PTW model parameters used for this transition region. For the half-hard copper in this experiment, the default parameters from annealed copper together with the thermally activated regime parameters fit to half-hard copper had the strength already transitioning to the much stronger phonon drag regime when the strain rates exceeded 10^6/s giving an initial yield strength of approximately 1600 MPa at a strain rate of 5.0×10^6/s.

A simple approach was used to modify PTW. The 520 MPa estimated strength, in spite of representing only a time and spatial average of strength, was used to modify two PTW parameters, y_1 and y_2, such that the yield strength passed approximately through 520 MPa at the strain rates between 1.5×10^6/s and 6.0×10^6/s that were estimated for the experiment. The PTW model was not affected at lower rates. Effectively, this modification extended the thermally-activated regime strengths until the rates exceed about 10^7/sec. Figure 7 shows the simulation results with the new PTW model, and the agreement with data is excellent. The simulations indicate that the total plastic strain reaches about 90% in the spike for $\eta_0 k$ = 0.45. Nonetheless, calculations indicate that the velocity predictions are more sensitive to yield stress than to saturation stress, as has been observed before [13]. Therefore, the saturation stress in the model was not modified. Note that Rayleigh Taylor instability experiments have also been used to constrain PTW models in a similar strain rate regime [32].

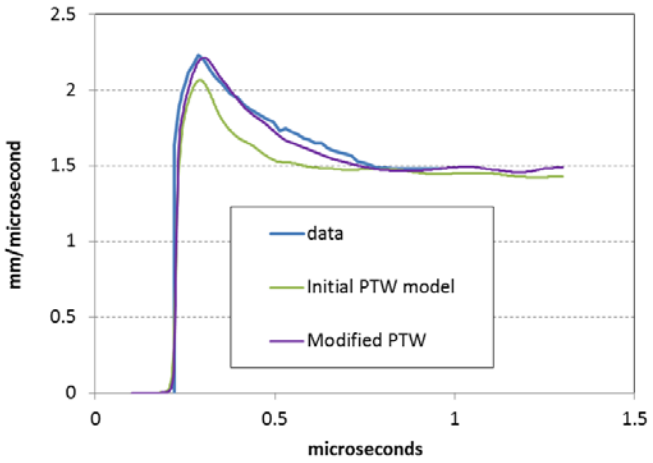

Figure 7. The modified PTW strength model fits the data very well.

Conclusions

RMI experiments on Cu were used modify a PTW constitutive model in the regime between 10^4/s and 10^7/s, where experimental data to constrain the model were lacking. The improved PTW model reproduces the experimental data quite well. This result is one indication that RMI experiments can be quite sensitive to material strength in a high strain rate regime that is difficult to otherwise access.

Table 1 summarizes the discussion in the Introduction about instability experiments used to infer material strength. Although they all access similar strain rates, up to about 10^7/s, there are significant differences between RT experiments and the two types of RMI experiments. RT experiments are shockless and RMI experiments involve a shock. Compared to the other two, the RMI experiment in the free surface configuration (A_t = -1) tests strength at lower pressure following a shock and release, and is the easiest to field experimentally because it can be diagnosed without radiography. In the other two configurations, instabilities evolve at higher pressures. To our knowledge, no RMI experiment in the Atwood = +1 configuration has ever been reported, presumably because of the difficulty of fabricating pieces with mating perturbations, and the difficulty with diagnosing the growth- and strain-rates. The RMI experiment in the free surface configuration can be successfully diagnosed without radiography, which makes experiments much simpler and less expensive.

Table 1. Comparing different types on dynamic instability-based experiments that can be used to infer strength at very high rates.

	Rayleigh-Taylor	Richtmyer-Meshkov Atwood = +1	Richtmyer-Meshkov Atwood = -1
Acceleration	Shockless	Shock	Shock
Strain rate	High	High	High
Pressure	High (confined)	High (confined)	Low (free surface releases)
Diagnostics	Radiography	Radiography	Surface velocimetry (radiography can be added)
Measured behavior	Growth rate	Arrest – final spike height	Arrest – final spike height

ACKNOWLEDGEMENTS

We acknowledge the support of the pRad team in acquiring these data.In addition, we appreciate contributions to these experiments by members of the LANL MST-7 group where our Cu targets were machined and characterized by F. Garcia, B. Day and D. Schmidt.

This work was performed at Los Alamos National Laboratory, operated by the Los Alamos National Security, LLC for the National Nuclear Security Administration of the U.S. Department of Energy under contract DE-AC52-06NA25396. By acceptance of this article, the publisher recognizes that the U.S. Government retains a nonexclusive, royalty-free license to publish or reproduce the published form of this contribution, or to allow others to do so, for U.S. Government purposes.

REFERENCES

1. Barnes JF, Blewett PJ, McQueen RG, Meyer KA, Venable D (1974) Taylor instability in solids. J Appl Phys 45 (2):727-732. doi:doi:http://dx.doi.org/10.1063/1.1663310
2. Colvin JD, Legrand M, Remington BA, Schurtz G, Weber SV (2003) A model for instability growth in accelerated solid metals. J Appl Phys 93 (9):5287-5301. doi:doi:http://dx.doi.org/10.1063/1.1565188
3. Lebedev AI, Nizovtsev PN, Rayevsky VA, Solovyov VP Rayleigh–Taylor Instability in Strong Media, Experimental Study. Young R, Glimm J, Boston B (eds) Proceedings of the Fifth International Workshop on Compressible Turbulent Mixing, 1996.
4. Barton NR, Bernier JV, Becker R, Arsenlis A, Cavallo R, Marian J, Rhee M, Park H-S, Remington BA, Olson RT (2011) A multiscale strength model for extreme loading conditions. J Appl Phys 109 (7):073501. doi:doi:http://dx.doi.org/10.1063/1.3553718
5. Smith RF, Eggert JH, Rudd RE, Swift DC, Bolme CA, Collins GW (2011) High strain-rate plastic flow in Al and Fe. J Appl Phys 110 (12):123515. doi:doi:http://dx.doi.org/10.1063/1.3670001
6. Piriz AR, Cela JJL, Tahir NA, Hoffmann DHH (2008) Richtmyer-Meshkov instability in elastic-plastic media. Phys Rev E 78 (5):056401
7. Piriz AR, Cela JJL, Tahir NA (2009) Richtmyer–Meshkov instability as a tool for evaluating material strength under extreme conditions. Nucl Instrum Meth A 606 (1):139-141
8. Dimonte G, Terrones G, Cherne FJ, Germann TC, Dupont V, Kadau K, Buttler WT, Oro DM, Morris C, Preston DL (2011) Use of the Richtmyer-Meshkov instability to infer yield stress at high-energy densities. Phys Rev Lett 107 (26):264502
9. Buttler WT, Oró DM, Preston DL, Mikaelian KO, Cherne FJ, Hixson RS, Mariam FG, Morris C, Stone JB, Terrones G, Tupa D (2012) Unstable Richtmyer-Meshkov growth of solid and liquid metals in vacuum. J Fluid Mech 703:60-84
10. López Ortega A, Lombardini M, Pullin DI, Meiron DI (2014) Numerical simulations of the Richtmyer-Meshkov instability in solid-vacuum interfaces using calibrated plasticity laws. Phys Rev E 89 (3):033018
11. Mikaelian KO (2013) Shock-induced interface instability in viscous fluids and metals. Phys Rev E 87 (3):031003
12. Plohr JN, Plohr BJ (2005) Linearized analysis of Richtmyer-Meshkov flow for elastic materials. J Fluid Mech 537:55-89
13. Prime MB, Vaughan DE, Preston DL, Buttler WT, Chen SR, Oró DM, Pack C (2014) Using growth and arrest of Richtmyer-Meshkov instabilities and Lagrangian simulations to study high-rate material strength. Journal of Physics: Conference Series 500 (11):112051
14. Buttler WT, Oro DM, Preston D, Mikaelian KO, Cherne FJ, Hixson RS, Mariam FG, Morris CL, Stone JB, Terrones G, Tupa D (2012) The study of high-speed surface dynamics using a pulsed proton beam. AIP Conference Proceedings 1426 (1):999-1002. doi:doi:http://dx.doi.org/10.1063/1.3686446
15. Asay JR, Mix LP, Perry FC (1976) Ejection of material from shocked surfaces. Applied Physics Letters 29 (5):284-287. doi:doi:http://dx.doi.org/10.1063/1.89066
16. Germann TC, Hammerberg JE, Holian BL (2004) Large-Scale Molecular Dynamics Simulations of Ejecta Formation in Copper. AIP Conference Proceedings 706 (1):285-288. doi:doi:http://dx.doi.org/10.1063/1.1780236
17. Zellner MB, Buttler WT (2008) Exploring Richtmyer–Meshkov instability phenomena and ejecta cloud physics. Applied Physics Letters 93 (11):114102. doi:doi:http://dx.doi.org/10.1063/1.2982421
18. Zellner MB, Dimonte G, Germann TC, Hammerberg JE, Rigg PA, Stevens GD, Turley WD, Buttler WT (2009) INFLUENCE OF SHOCKWAVE PROFILE ON EJECTA. AIP Conference Proceedings 1195 (1):1047-1050. doi:doi:http://dx.doi.org/10.1063/1.3294980
19. Dimonte G, Terrones G, Cherne FJ, Ramaprabhu P (2013) Ejecta source model based on the nonlinear Richtmyer-Meshkov instability. J Appl Phys 113 (2):024905. doi:doi:http://dx.doi.org/10.1063/1.4773575
20. King NSP, Ables E, Adams K, Alrick KR, Amann JF, Balzar S, Barnes Jr PD, Crow ML, Cushing SB, Eddleman JC (1999) An 800-MeV proton radiography facility for dynamic experiments. Nucl Instrum Meth A 424 (1):84-91

21. Holtkamp DB Survey of optical velocimetry experiments-applications of PDV, a heterodyne velocimeter. Kiuttu GF, Turchi PJ, Reinovsky RE (eds) 2006 International Conference on Megagauss Magnetic Field Generation and Related Topics, Santa Fe, NM, 2006. IEEE, pp 119-128. doi:10.1109/MEGAGUSS.2006.4530668
22. Caramana EJ, Burton DE, Shashkov MJ, Whalen PP (1998) The Construction of Compatible Hydrodynamics Algorithms Utilizing Conservation of Total Energy. J Comput Phys 146 (1):227-262. doi:http://dx.doi.org/10.1006/jcph.1998.6029
23. Burton DE, Carney TC, Morgan NR, Runnels SR, Sambasivan SK, Shashkov MJ (2011) A cell-centered Lagrangian hydrodynamics method for multi-dimensional unstructured grids in curvilinear coordinates with solid constitutive models. Los Alamos National Laboratory Report Report LA-UR-11-04995
24. Dobratz BM, Crawford PC (1985) LLNL Explosives Handbook. Properties of chemical explosives and explosive simulants. Lawrence Livermore National Laboratory Report UCRL-52997 Change 2
25. Lyon SP, Johnson JD (1992) Sesame: the Los Alamos National Laboratory equation of state database. Los Alamos National Laboratory Report LA-UR-92-3407
26. Preston DL, Tonks DL, Wallace DC (2003) Model of plastic deformation for extreme loading conditions. J Appl Phys 93 (1):211-220
27. Tonks D, Zurek A, Thissell W, Vorthman J, Hixson R (2002) The Tonks ductile damage model. Los Alamos National Laboratory Report LA-UR-03-0809
28. Zurek AK, Thissell WR, Johnson JN, Tonks DL, Hixson R (1996) Micromechanics of spall and damage in tantalum. Journal of Materials Processing Technology 60 (1–4):261-267. doi:http://dx.doi.org/10.1016/0924-0136(96)02340-0
29. Tonks DL (1994) Percolation wave propagation, and void link-up effects in ductile fracture. Le Journal de Physique IV 4 (C8):C8-665-C668-670
30. Tonks DL, Zurek AK, Thissell WR (2002) Void Coalescence Model for Ductile Damage. AIP Conference Proceedings 620 (1):611-614. doi:doi:http://dx.doi.org/10.1063/1.1483613
31. Tonks DL, Bronkhorst CA, Bingert JF (2011) Inertial Effects In Dynamical Ductile Damage in Copper. Los Alamos National Laboratory Report LA-UR-11-05803
32. Park H-S, Lorenz KT, Cavallo RM, Pollaine SM, Prisbrey ST, Rudd RE, Becker RC, Bernier JV, Remington BA (2010) Viscous Rayleigh-Taylor Instability Experiments at High Pressure and Strain Rate. Phys Rev Lett 104 (13):135504